Crop Protection 110 (2018) 65–72

Contents lists available at ScienceDirect

Crop Protection

journal homepage: www.elsevier.com/locate/cropro

Inter-seasonal and altitudinal inoculum dynamics for wheat stripe rust and powdery mildew epidemics in Gangu, Northwestern China

Yilin Gu, Yong Li, Cuicui Wang, Bingyao Chu, Qi Liu[1], Yong Luo[*,2], Zhanhong Ma[**]

Department of Plant Pathology, The Key Laboratory of China Ministry of Agriculture, China Agricultural University, Beijing 100193, China

ARTICLE INFO

Keywords:
Airborne spore dynamic
Puccinia striiformis f. sp. *tritici*
Blumeria graminis f. sp. *tritici*
Duplex real-time PCR

ABSTRACT

Inter-seasonal and altitudinal dynamics of airborne spores of wheat stripe rust and powdery mildew pathogens were studied in northwestern China (Gangu, Gansu) in this study. Burkard spore traps were placed in three locations of Gansu county of the Gansu province at various altitudes, named South mountain, Valley and North mountain. Airborne spore samples were collected from March 2013 to December 2015, totaling 1365 collections for each pathogen. The airborne spore concentration of both pathogen, quantified using duplex real-time PCR assay, were consistently higher in the spring and summer than in fall and winter seasons. The within-crop season airborne inoculum levels were associated with disease severity levels. No difference was found in the Area Under the Spore Concentration Progress Curve (AUSCPC) between spring and summer for both pathogens as well as among the three locations, and there was significant correlation of ten-day spore concentrations between any two of the three locations. Our findings suggest that Gangu is an important source of oversummering inoculum for both diseases with frequent exchange of airborne spores within this region. The time-series analysis demonstrated that the airborne spore concentrations of *Pst* for all the 10-day-spore-sum during 3 years at three locations were all significantly described by the Autoregressive Integrated Moving-Average (ARIMA) (1, 0, 0) models, while, those of *Bgt* fitted different models, which contributed to predicting the tendency of airborne spore concentrations for both pathogens in Gangu.

1. Introduction

Stripe rust, caused by *Puccinia striiformis* Westend. f. sp. *tritici* Eriks. (*Pst*), is a devastating foliar disease of wheat worldwide (Chen, 2005; Chen et al., 2014), particularly in China, given the large extension of epidemics resulting in significant yield loss (Wan et al., 2004, 2007; Zeng and Luo, 2006). In China, epidemics depend extensively on pathogen migration and long-distance dispersal (Zeng and Luo, 2006). Thus, sources of initial inoculum for epidemics can be either exogenous or endogenous depending on ecological features, and knowledge about potential sources and timing of inoculum release are important to design regional disease management strategies. Although the sexual stage of *Pst* had been proved to occur naturally (Zhao et al., 2013), urediniospores seem to play a critical role in stripe rust epidemics in China (Chen et al., 2014). Northwestern regions of China were considered as main sources of initial inoculum for early season epidemics in eastern China due the ability of *Pst* to oversummer (Li and Zeng, 2002).

Tianshui is located in mountainous area of Gansu Province at the altitude ranging from 800 m to 2400 m above sea level (asl). The topographic and climatic diversity and distribution of various wheat cultivation systems from low to high altitudes in this area favor inoculum survival and epidemic development (Li and Zeng, 2002; Zhang and Li, 1991). Gangu County of Tianshui has been considered as the most important location, providing significant amount of inoculum to initiate nationwide stripe rust epidemics (Zeng and Luo, 2006). Wheat-growing seasons during winter and spring overlap among different altitudes and volunteer plants can be found at different periods of time, thus serving as a bridge for the pathogen to cross summer and infect plants during the fall at other locations (Zeng and Luo, 2006). Vertical (altitudinal) dispersal of spores is assumed to occur and potentially play an important role in pathogen oversummering and overwintering due to cool summer at high altitude and mild winter at low altitude. However, direct evidence of the year-round presence of airborne spore across different altitudes is lacking and the knowledge could lead to improved understanding of the aerobiology and risk of epidemic onset at different time periods.

* Corresponding author.
** Corresponding author.
E-mail addresses: ygluo@ucanr.edu (Y. Luo), mazh@cau.edu.cn (Z. Ma).
[1] Current address. College of Agronomy, Xinjiang Agricultural University, Urumqi 830052, China.
[2] Current address. University of California, Kearney Agricultural Research and Extension Center, Parlier CA 93648, USA.

https://doi.org/10.1016/j.cropro.2018.03.005
Received 17 November 2017; Received in revised form 22 January 2018; Accepted 14 March 2018
Available online 10 April 2018

Powdery mildew, caused by *Blumeria graminis* (DC.) Speer f. sp. *tritici* Marchal. (*Bgt*), is increasing in importance for wheat crops in China due to significant yield loss (Cao et al., 2016; Zeng et al., 2010). Since 2001, the disease occurred in 6–8 million hectares of wheat in China (Zheng et al., 2013). Furthermore, the pathogen is capable of long distance dispersal (Limpert et al., 1999) and it has been found to complete its life cycle in Gangu (Li et al., 2013), potentially serving as initial source of inoculum for epidemics on seedlings during the fall season. Previous studies showed that the ability of powdery mildew pathogen to overwinter in diseased leaves or wheat debris in most wheat-growing regions in China (Liu and Shao, 1998), but its ability to oversummer in western regions, build up inoculum during the summer period and disperse long-distance are still unclear. Although both conidia and ascospores of *Bgt* both could serve as initial inoculum, the conidia played a much more prominent role than ascospores did on disease development (Cao et al., 2011; Liu and Tang, 1985; Zheng et al., 2013).

Therefore, knowledge of the inter-seasonal inoculum dynamics of both *Pst* and *Bgt* in this region is needed. For instance, the questions about year-round airborne spore dynamics and the possible relationship of spore dynamics among different altitudes in this region still need answers. Importantly, we still didn't know the possible amount of airborne spores out of the wheat-growing season in summer. We also had no clue about the possible existence, as well as the amount, of the inoculum during the winter in this region.

Using spore traps to monitor airborne inoculum and to answer above questions is an applicable approach in epidemiological research. Burkard spore trap (Aylor, 1993; Kennedy and Wakeham, 2015) is an efficient tool to collect airborne spores. However, the traditional approach to quantify spore concentration by microscopic counting is time consuming and labor intensive. Real-time quantitative PCR (*q*PCR) approach had been widely used in epidemiological studies to quantify plant pathogen spores and to predict plant disease developments (Luo et al., 2007; Meitz-Hopkins et al., 2014; West and Kimber, 2015), including wheat stripe rust (Dedeurwaerder et al., 2011) and powdery mildew (Cao et al., 2016). Duplex quantitative PCR allows simultaneous quantification of two different targets (pathogens) (Bernal-martínez et al., 2012; Yang et al., 2015).

The objectives of this study were to (i) monitor the intra and inter-seasonal fluctuation patterns of airborne spore concentrations of *Pst* and *Bgt*, (ii) analyze the relationship between the Area Under the Spore Concentration Progress Curve (AUSCPC) and the Area Under the Disease Progress Curve (AUDPC) of disease index recorded at different developmental stages, and (iii) compare spore concentrations at three altitudes.

2. Materials and methods

2.1. Study area

The Weihe River crosses Gangu County from west to east, and splits this mountainous area into three parts: South mountain, Valley and North mountain. Air humidity generally decreases from south to north, and temperature declines with increasing of altitude. In this study, three representative locations were selected and spore traps were placed at three altitudes (Fig. 1): 1730 m asl at South mountain

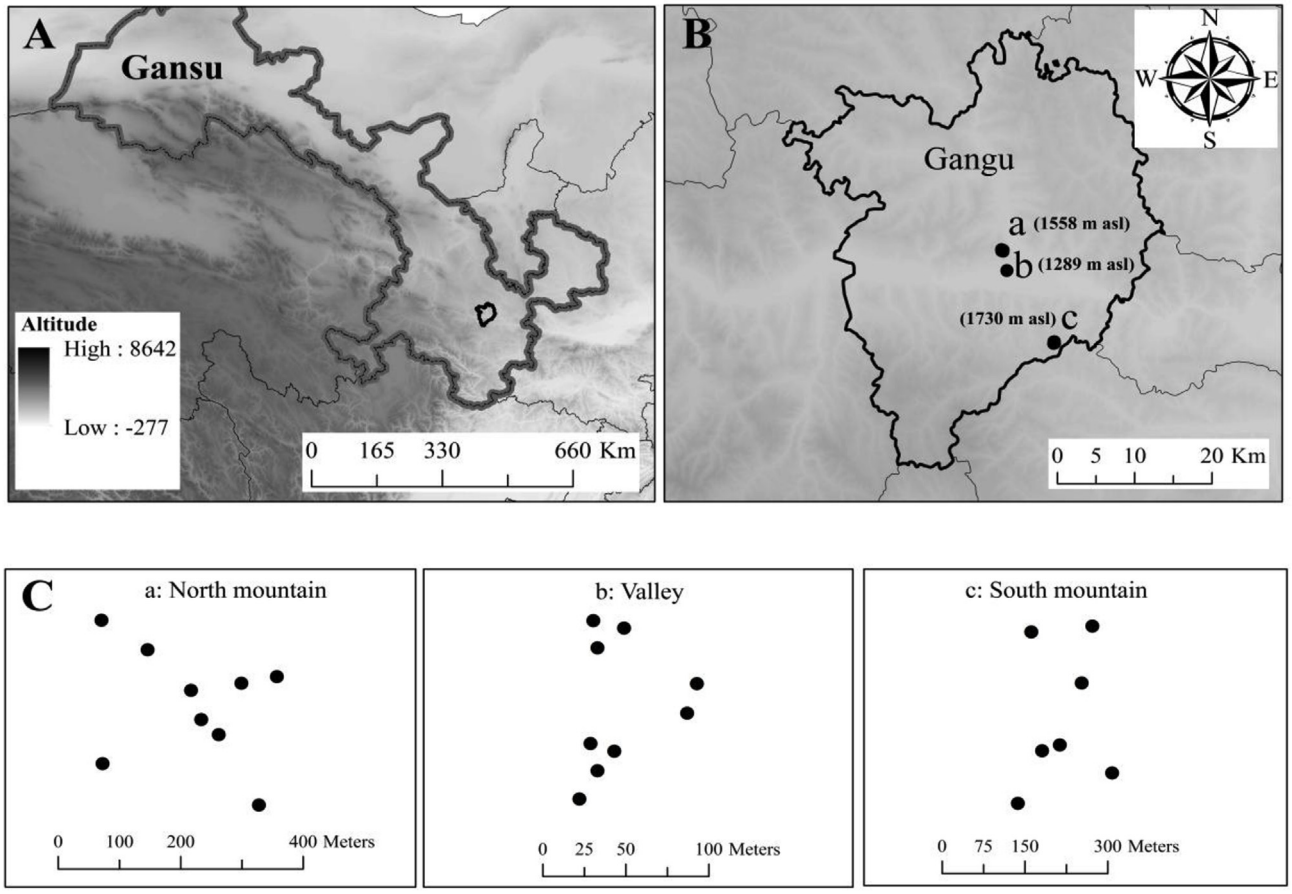

Fig. 1. The locations where the spore traps were placed and the wheat fields for disease assessment of stripe rust and powdery mildew used in this study. A: Map showing the location of Gangu county within Gansu province and the topology of the surrounding area. B: Three locations in Gangu county where spore traps were placed: a: North mountain, b: Valley, and c: South mountain. C: Distribution of the wheat fields used for disease assessment of stripe rust and powdery mildew at three locations involved in this study. Each dot represents a wheat field with about 200–600 m^2.

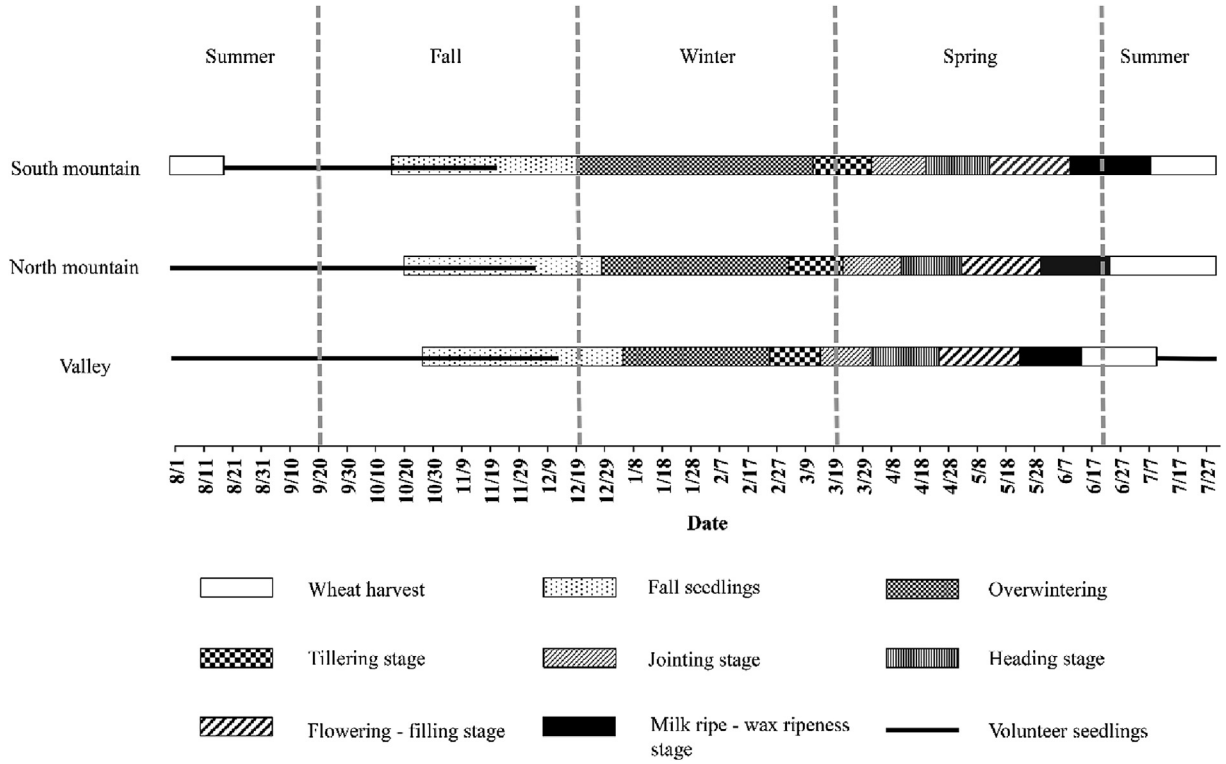

Fig. 2. Comparison of wheat growing seasons among the three locations of Gangu involved in this study.

(Location SM, 105.36235° E and 34.67403° N), 1289 m asl in Valley (Location VL, 105.29144° E and 34.76281° N), and 1558 m asl at North mountain (Location NM, 105.28709° E and 34.78568° N). Wheat is planted around these locations. Epidemics of stripe rust and powdery mildew are typically observed in these three locations. The wheat-growing season spans from October to June of the following year, and volunteer plants usually grow in summer and fall (Fig. 2), overlapping with the period of fall wheat seedlings. The altitude gradually decreases from South mountain to Valley, and the period of overlapping of wheat with volunteer seedlings varied at different altitudes (Fig. 2).

2.2. Spore trapping and sample collection

Three Burkard Automatic Multi-Vial Cyclone samplers (Burkard Manufacturing Co. Ltd., UK) for field operation were used. These spore traps can collect airborne particles directly into 1.5 ml Eppendorf tubes. The air throughput of spore trap is 16.5 L/minute, which is 23.76 m^3/day. The spore traps run 24 h for each sample, and four samples were collected per week (every Tuesday, Thursday, Saturday and Sunday). The tubes were replaced every two weeks. A wing on the spore trap was used to ensure that the inlet orifices always face to the direction of the wind. The spore traps were placed approximately 3 m above ground in order to facilitate management and avoid the contamination by splash-dispersed spores during rain. The spore trapping was performed from March 2013 to December 2015 at the SM, from April 2013 to December 2015 at the NM and VL. Spore trap samples were stored at −20 °C before processing.

2.3. DNA extraction

Spore trap samples were processed to extract DNA using PowerSoil® DNA Isolation Kit (MO BIO Laboratories, Inc., USA) by following the protocols from manufacturer. To collect all the spores in the sample, the 500 µl upper part of reagent solution in PowerBead Tubes was transferred into the Eppendorf tubes which contained the spore trap samples. The Eppendorf tubes were shaken on the Vortex Genin (Scientific Industries, USA) for 2 min to acquire the spore suspension. The spore suspension was then transferred into the PowerBead tubes, added 60 µl of Solution C1, preheated at 60 °C until dissolved, and inverted several times to mix. The PowerBead Tubes were processed with a FastPrep-24 Instrument (MP Biomedicals, LLC, USA) twice each for 40 s at 6.0 m/s with an interval of a 5 min incubation in ice. The subsequent steps were operated following the instruction from the manufacture. Finally, 100 µl DNA extracts were obtained and stored at −20 °C for later use.

2.4. Quantification of airborne spore concentration

Two sets of primer pairs and *Taq*Man probes specific to *Pst* and *Bgt* based on the ribosomal DNA internal transcribed spacer (ITS) sequences, respectively (Li et al., 2015), were used in this study. The sequences of primers for *Pst* were *Pst*-F (5′ - AACCCTCTCATTAAATAA TTTTG - 3′), and *Pst*-R (5′ - CCAACTTATAGAAAAGTGACTTA - 3′), and that of the corresponding probe was *Pst*-P (5′ - FAM - ATTACAGCAGC ACTCAACATCCATT - BHQ1 - 3′). The sequences of primers for *Bgt* were *Bgt*-F (5′ - CCGTAACAACCTCTCAAG - 3′), and *Bgt*-R (5′ - CAACCTGA GCAATTAAGGA - 3′), and that of the corresponding probe was *Bgt*-P (5′ - HEX - TATTGGGACTCGCTGCCTC - BHQ1 - 3′).

A duplex one-tube real-time *q*PCR method to quantify the number of spores for *Pst* and *Bgt* in the air samples was previously developed and optimized (Li et al., 2015). The amplifications were performed with a MyiQ™2 Two Color Real-Time PCR Detection System (Bio-Rad Laboratories, USA) in a 20 µl volume containing 2.00 µl of 10 × PCR buffer, 3.20 µl (25 µM) of $MgCl_2$, 2.00 µl (2500 µM) of dNTP, 0.30 µl of each primer (10 µM), 0.25 µl of each probe (10 µM), 0.60 µl of r*Taq* (5 U/µL), 8.80 µl of ddH_2O, and 2.00 µl of DNA template. All of the reagents were purchased and the primers and probes were also synthesized from TAKARA (TAKARA Biotechnology (Dalian) Co., LTD., China). The *q*PCR condition was initiated with denaturation at 95 °C for 3 min, followed by 40 cycles of denaturation at 94 °C for 20 s, annealing at 55 °C for 30 s, extension at 72 °C for 30 s. The fluorescence signals from the probes were recorded at 72 °C during every cycle. Each sample was run for three replicates and the average Ct value of each sample

was calculated, the DNA of *Pst* and *Bgt* was used as positive control and the ddH_2O was used as negative control.

After the *q*PCR, the numbers of spores of the two pathogens for each sample were calculated based on the corresponding average Ct values from three replicates and by using the corresponding standard curves. The corresponding standard curves were: $y = -0.31\ x + 11.74$ ($R^2 = 0.98$, $P < 0.01$) for *Pst*, and $y = -0.28\ x + 10.66$ ($R^2 = 0.99$, $P < 0.01$) for *Bgt,* where x is average Ct value and y is $\log_{10}$ (number of spores) (Li et al., 2015). Thus, the airborne spore concentration was estimated for each sampling date. The year-round spore dynamic curve described as $\log_{10}$ (number of spores/100 m^3 air) versus sampling date was generated for each pathogen.

2.5. Disease assessment

Seven to nine fields at a distance less than 1 km away from each air sampling site were selected for disease assessment (Fig. 1). The fields of SM and NM had no irrigation system while those in VL used light irrigation. No fungicides were applied in any of the fields. Wheat stripe rust and powdery mildew were periodically recorded during the growing season (March to June). Stripe rust and powdery mildew assessments were conducted at least three sequential times in a season. On each disease assessment date, five spots of each farmer's field were randomly selected, and 20 plants were used to record the disease incidence (DI, DI = number of diseased leaves/number of total leaves), and disease severity (DS), as well as the corresponding growth stage. The disease severity of stripe rust was assessed according to the proportion of diseased leaf area of the whole leaf area (Shang et al., 1990), and that of powdery mildew was assessed with a '0–9' scale based on the number and size of lesions on wheat leaves (Sheng and Duan, 1991). The growth stages of wheat were recorded according to Zadoks et al. (1974). The disease index (DX) was calculated as DX = DI × DS (Zeng and Luo, 2006). The disease development curve as description of DX versus disease recording date was generated for each case.

2.6. Data analyses

The variable A_{rea} represents either the Area Under the Disease Progress Curve (AUDPC), or the Area Under the Spore Concentration Progress Curve (AUSCPC) concentration of either of the two diseases. It was calculated with the following formula:

$$\text{Area} = \sum_{i}^{n} \left[\left(\frac{x_i + x_{i+1}}{2} \right) (t_{i+1} - t_i) \right]$$

where x_i is disease index or spore concentration on the ith day, t_i is the ith day for disease assessment or spore trapping, n is the total number of time for disease recording or spore trapping.

All the statistical analyses were performed with Statistical Product and Service Solutions (SPSS, version 20.0, IBM, USA). In further data analysis, the annual spore concentration data were split into four seasons, March 21 – June 20, June 21 – September 20, September 21 – December 20, and December 21 – March 20, to approximately represent spring, summer, fall and winter for each year. Considering the wide range of spore concentrations, the log-transformed AUSCPC was calculated. Homogeneity of variances was confirmed by using the Levene' tests with SPSS, and then the one-way ANOVA was performed. Comparisons in AUSCPC among different seasons for each year and among different locations for each of the two pathogens were conducted followed by multiple comparison tests (Fisher's least significant difference, LSD) of means with significance level of $P = 0.05$.

For each of the two diseases, the correlation between the AUSCPC and the AUDPC of disease index in corresponding growing season was analyzed using Pearson's correlation coefficients with SPSS.

In order to determine the relationship in spore concentration between any two of the three locations, we used 10-day-spore-sum as a variable in analysis. This variable was calculated by summing spore concentration for every 10 days starting from March 1, 2013 to December 31, 2015 for each location. The same correlation method as described above was performed using the multi-year data of this variable for each location and each of the two diseases.

The time-series analysis was conducted to explore the natural characteristics of temporal variation in the airborne spore concentration of 10-day-spore-sum (calculated from March 1, 2013 to December 31, 2015) using SPSS software, and autoregressive integrated moving-average (ARIMA) models, an approach of time series analysis used to describe a wide range of time series and periodic patterns, were built for each location and each disease. The model was used to reveal the periodic patterns of dynamics of airborne spore. The correlations between the fitted and the observed spore concentration were analyzed with Pearson's correlation coefficients implemented in SPSS.

3. Results

3.1. Annual dynamics of airborne spore concentration

Fig. 3 shows the annual dynamics of spore concentration of *Pst* for each of the three locations in this study. In general, the spores were detected during the whole year at all three locations. The spore concentrations among the three locations were similar in general during a year. The overall range of spore concentration was from 0 to 10,000 spores/100 m^3 air. However, the highest spore concentrations appeared during the wheat growing season from March to June, and lowest ones appeared in the winter. Compared with *Pst,* quite similar patterns of annual dynamics of spore concentration for *Bgt* were observed (Fig. 3).

3.2. Seasonal pattern of AUSCPC for both pathogens

The Levene's tests showed the homogeneity of variance for all the means tested at the significance levels greater than 0.05. Similar patterns of AUSCPC of *Pst* were observed among the three years (Fig. 4). There were no significant differences in AUSCPC between spring (March 21 to June 20) and summer (June 21 to September 20) seasons, or between summer and fall (September 21 to December 20) seasons. The airborne spore concentration was reduced significantly in winter in 2013, but not in 2014 (with missing data of 2015) (Fig. 4).

Comparison of $\log_{10}$ (AUSCPC) of *Pst* showed no difference among three locations for each of the four seasons (Fig. S1). The same results were also observed for *Bgt*, showing no difference in $\log_{10}$ (AUSCPC) of spore concentration among the three locations for each of the four seasons (Fig. S2).

However, the different patterns of airborne spore dynamics among seasons for *Bgt* were observed (Fig. 4). Across the three years, the highest spore concentrations were observed in spring, followed by those in summer and fall. The spore concentrations decreased to the lowest levels in winter. Thus, the clear trend of decrease in spore concentration from the spring to the winter was observed. The results demonstrated that although the airborne spores of *Bgt* were observed in whole year, their amounts during the four seasons were quite different. Namely, the highest airborne spore concentrations occurred during the wheat growing season, while those out of season were significantly reduced.

3.3. Correlation between disease development and spore concentrations

To determine the relationship of spore concentration among different locations, the correlations in 10-day spore concentration between any two of the three locations were analyzed for both *Pst* and *Bgt*. The result showed the significant correlations in spore concentration between any two locations for both pathogens (Table 1).

Similar patterns of the disease index for both pathogens among three locations during 2013–2015were observed, except for that of North mountain in 2014 (Fig. S3). The correlations between the

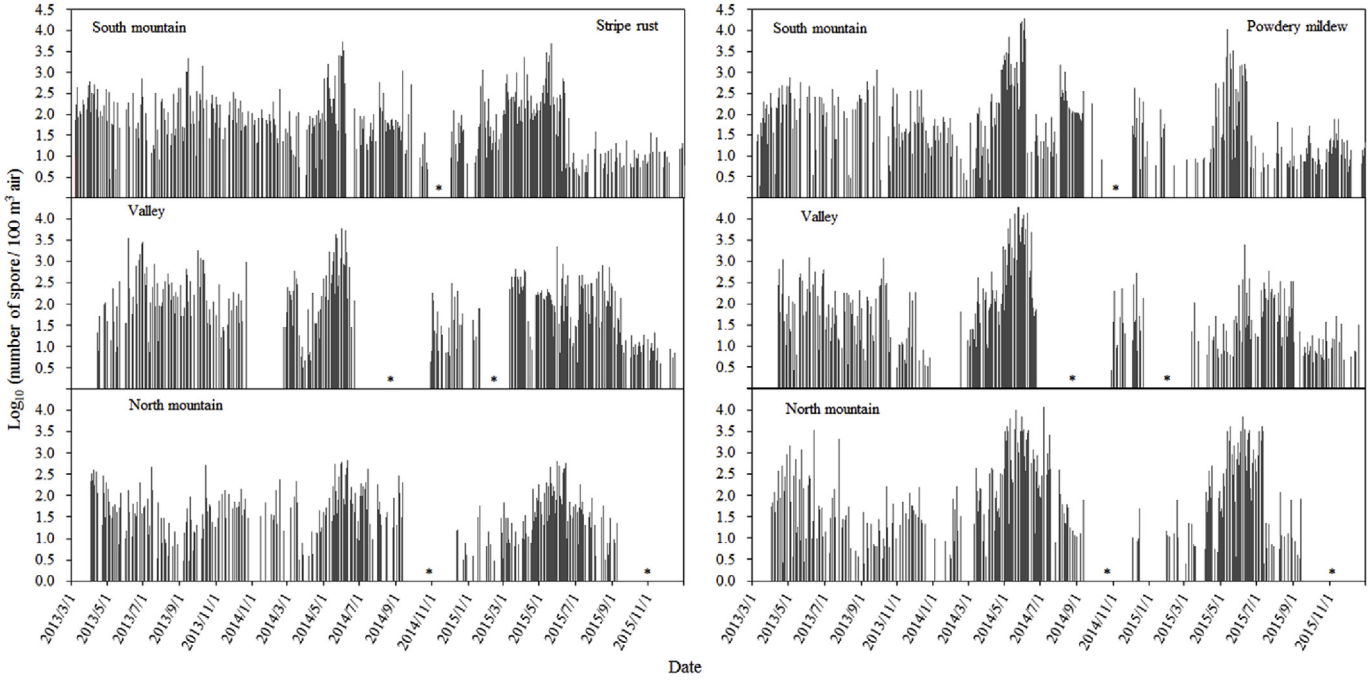

Fig. 3. The annual dynamics of airborne spore concentration ($\log_{10}$ (spores/100 m^3)) of *Puccinia striiformis* f. sp. *tritici* (*Pst*) and *Blumeria graminis* f. sp. *tritici* (*Bgt*) at the three locations used in this study during 2013–2015. * indicates a period of missing data due to failure of spore traps. These periods include Oct. 24 - Dec. 1, 2014 for South mountain, Dec. 25, 2013–Feb. 14, 2014, Jun. 23 – Oct. 27, 2014 and Feb. 20 – Mar. 11, 2015 for Valley, and Sep. 12 – Dec. 1, 2014 and Sep. 14 – Dec. 31, 2015 for North mountain.

AUSCPC and the AUDPC of disease index were all significant at $P < 0.05$ for both diseases (Table 2).

3.4. Time-series analysis for spore concentrations

The airborne spore concentrations of *Pst* for all the 10-day-spore-sum during 3 years at three locations were all significant as described by the ARIMA (1, 0, 0) models, and those of *Bgt* were different (Table 3). All of the models were significant, and the parameters estimates were all significant at $P < 0.05$. The correlation coefficients between the fitted and the observed airborne spore concentration of *Pst* were 0.5043, 0.4835 and 0.5758 for SM, VL and NM, and those of *Bgt* were 0.5817, 0.7145 and 0.6254 for SM, VL and NM, respectively, at $P < 0.01$.

4. Discussion

Based on multi-environment data, this study found that the airborne spores of both *Pst* and *Bgt* existed year-round in the studied region of Gansu Province. However, the spore concentrations in winter were lower than those in other three seasons for both the pathogens. This finding implied that the Gangu region could continuously provide inoculum of both pathogens, to eastern regions in China where the pathogens usually do not survive between wheat crops, which was intensively discussed by Zeng and Luo (2006). This finding also confirmed that the studied region of Gansu Province serves as an important area where both *Pst* and *Bgt* could successfully oversummer and overwinter (Li et al., 2013; Zeng and Luo, 2006) to complete their life cycles.

The reliability of prediction of plant disease epidemics by using spore trap results had been proved. For instance, Nagarajan et al. (1977) trapped the urediniospores from rain samples and showed that it could be used to predict the occurrence of wheat stem rust. Cao et al. (2015) built the cumulative logit models to describe the severity of wheat powdery mildew based on airborne conidial concentration and weather variables. They found that the airborne spores were the most important factor in disease development. Recently, the qPCR was used as replacement of traditional microscopic method for counting spores (Cao et al., 2016; Luo et al., 2007), and the method is a highly-efficient and stable (Dedeurwaerder et al., 2011; West et al., 2009). Meanwhile, using real-time PCR assays to process spore trap samples provided an efficient and accurate method for quantitative analysis of airborne inoculum of pathogens (Duvivier et al., 2013; Liu et al., 2015).

The information on annual spore dynamics of both pathogens is valuable to design the regional disease management strategies based on the clue of pathogen overwintering and oversummering features and dispersal directions among different regions. The goal of this study was to estimate future risk of disease development by using spore trap data. The significant correlations between AUSCPC and AUDPC of disease index for both diseases confirmed to achieve the goal of our study possibility. Further research is needed to generate methodology for such prediction approach. It is also important to use spore trap data to estimate the potential inoculum that may disperse eastward and to estimate the possible risk of epidemics of both diseases in eastern regions of China relying on a network of traps.

Zeng and Luo (2006) reviewed that the geological features of the Gangu showed the existence of wheat and volunteer seedlings in the fields in different seasons that the period of time overlapped at different altitudes in a year. Namely, the host plants for *Pst* and *Bgt* existed year-round to serve as basis for pathogen reproduction (Fig. 1). Especially, at high altitude with cooler climate (Zeng and Luo, 2006) where wheat growing season is longer than that at low altitudes, the pathogen survival and reproduction play more crucial role on disease development.

The higher spore concentrations of both pathogens during wheat growing stages from GS20 to GS80 than those of oversummering were detected. However, no statistical differences in AUSCPC between spring and summer seasons were observed for both pathogens. Additionally, there were no statistical differences in AUSCPC between summer and fall seasons. The results indicated that in the summer as out of wheat growing season, the airborne spore concentrations were still as high as those in the growing season, and we detected the over-summering airborne spores, namely, the pathogen could have the potential to

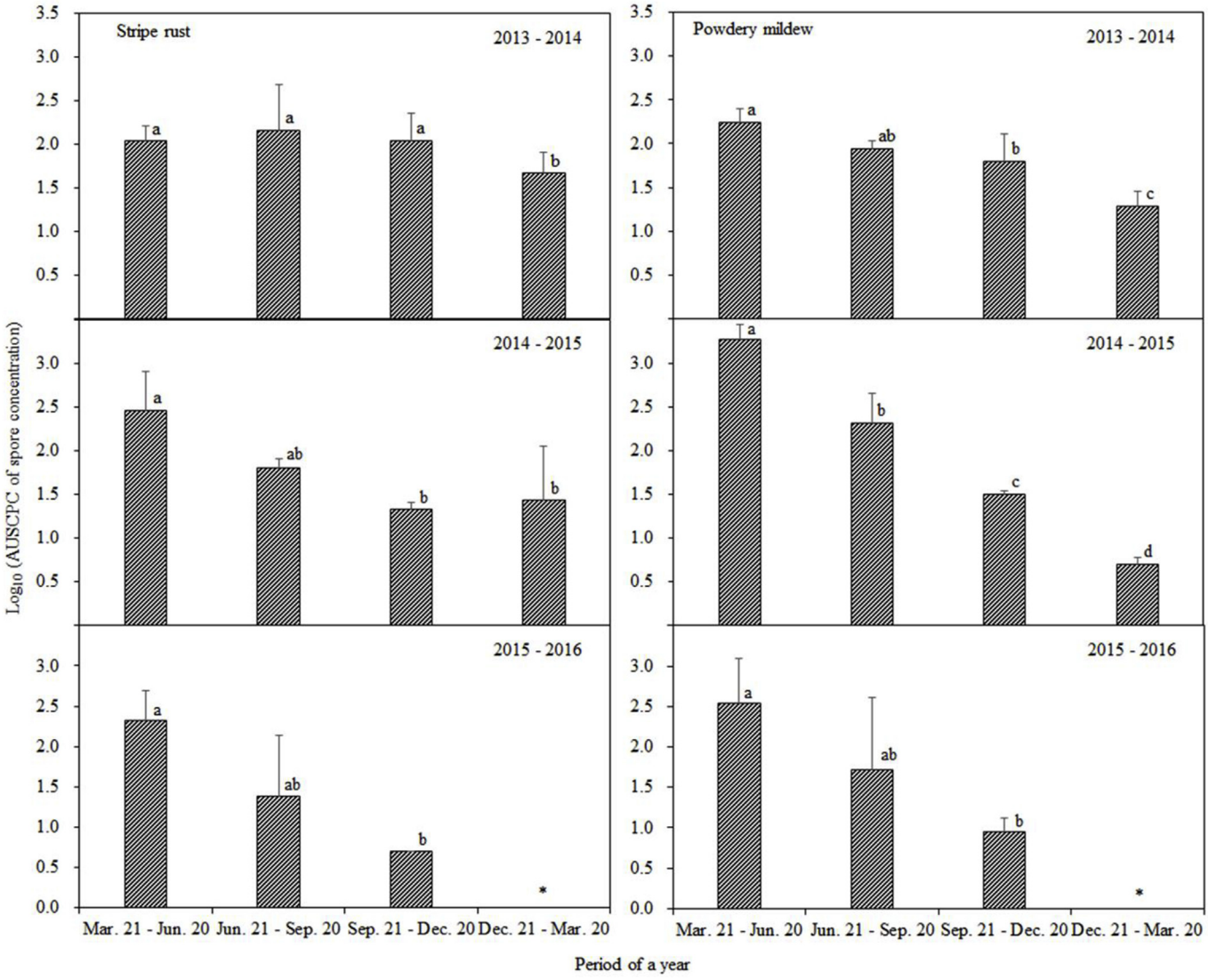

Fig. 4. The Area Under the Spore Concentration Progress Curves (AUSCPC) of *Puccinia striiformis* f. sp. *tritici* (*Pst*) and *Blumeria graminis* f. sp. *tritici* (*Bgt*) for the four seasons during each year. Each bar represents a mean value from three locations involved in this study. The different letters on top of the bars indicate the significant difference in mean values of the bars among different seasons at $P < 0.05$ based on multiple comparison tests (Fisher's least significant difference, LSD). *: Period of missing data because of spore trap failure.

Table 1
The correlations in the ten-day-spore-sum of *Puccinia striiformis* f. sp. *tritici* (*Pst*) and *Blumeria graminis* f. sp. *tritici* (*Bgt*) between any two locations involved in this study.

	South mountain	Valley	North mountain
Pst			
South mountain	–	0.722**	0.666**
Valley	0.722**	–	0.610**
Bgt			
South mountain	–	0.917**	0.682**
Valley	0.917**	–	0.632**

Ten-day-spore-sum was calculated by summing spore concentration for every 10 days starting from March 1, 2013 to December 31, 2015 for each location. * and ** mean the significance levels of correlation at $P < 0.05$ and $P < 0.01$, respectively.

survive the summer in this region. Because *Pst* could only over-summer on the volunteer seedlings at an altitude above 1700 m (Cao et al., 2011), and *Bgt* had a broader range of altitude for oversummering (Cao et al., 2011; Li et al., 2013), we inferred that the trapped spores likely came from the late-maturing wheat or volunteer seedlings at a higher altitude.

This study showed the similar trends of spore dynamics of *Pst* over seasons among the three locations. Based on the result of time-series analysis, such dynamics fitted well to the ARIMA (1, 0, 0) model in these locations, demonstrating a certain level of consistency among different altitudes. However, the situations of *Bgt* were different, and time-series analysis results showed that spore dynamics of different year's fitted different ARIMA models, which are helpful to understand the dynamic of airborne spores. Since the disease of stripe rust occurred earlier in South mountain than in other two locations in this study based on our observation and spore trap data, we inferred that South mountain could provide inoculum of stripe rust influencing location disease development.

Gansu Province is considered as an important region providing oversummering inoculum which disperses eastward to initiate inter-regional epidemics of wheat stripe rust (Zeng and Luo, 2006). Gangu is considered as a core region in Gansu where the amount of over-summering inoculum determines the intensity of disease epidemics in east regions of China. Additionally, the spores could also disperse to

Table 2
The correlation coefficients between the Area Under the Spore Concentration Progress Curves (AUSCPC) and the Area Under the Disease Progress Curve (AUDPC) of disease index for stripe rust and powdery mildew at three locations during. The data were obtained from the experiments during 2013 and 2015.

	South mountain	Valley	North mountain
Pst	0.664*	0.660*	0.980**
Bgt	0.856**	0.638**	0.855**

Note: * and ** mean the significance levels of correlation at $P < 0.05$ and $P < 0.01$, respectively.

Table 3
The time-series analysis for *Puccinia striiformis* f. sp. *tritici* (*Pst*) and *Blumeria graminis* f. sp. *tritici* (*Bgt*) based on all the data of 10-day-spore-sums for the three studied locations.

	Location	Model	Equation*	Significance
Pst	South mountain	ARIMA (1, 0, 0)	$Y_t = 8.4947 + 0.4949\ Y_{t-1} + \varepsilon_t$	0.9757
	Valley	ARIMA (1, 0, 0)	$Y_t = 11.7944 + 0.4661\ Y_{t-1} + \varepsilon_t$	0.9283
	North mountain	ARIMA (1, 0, 0)	$Y_t = 3.1353 + 0.6176\ Y_{t-1} + \varepsilon_t$	0.9984
Bgt	South mountain	ARIMA (2, 1, 1)	$Y_t = -0.6607\ Y_{t-1} - 0.3775\ Y_{t-2} + \varepsilon_t + 0.5172\ \varepsilon_{t-1}$	0.9400
	Valley	ARIMA (1, 0, 1)	$Y_t = 0.5625\ Y_{t-1} + \varepsilon_t + 0.3086\ \varepsilon_{t-1}$	1.0000
	North mountain	ARIMA (0, 0, 3)	$Y_t = 20.9193 + \varepsilon_t + 0.5452\ \varepsilon_{t-1} + 0.4449\ \varepsilon_{t-2} + 0.3363\ \varepsilon_{t-3}$	0.8975

The 10-day-spore-sum was calculated by summing spore concentration for every 10 days starting from March 1, 2013 to December 31, 2015 for each location. *: Y_t and Y_{t-1} are the 10-day-spore-sum at tth or t-1th time, respectively. The ε_t, ε_{t-1}, and ε_{t-2} are the white noises at tth, t-1th and t-2th time, respectively.

Northwestern regions such as Qinghai and Xinjing (Wan et al., 2015). Compared with the possibility of eastward and westward long-distance dispersal of airborne spores, the phylogenetic evidences showed that the exchange of inoculum between Gangu and Sichuan basin was frequent (Liang et al., 2016). In other words, the inoculum initiating spring epidemics in Sichuan basin was most likely from the fall seedlings in Gangu. Additionally, the pathogen population of *Pst* of Gangu was considered as the same as that of the adjacent Ningxia Province (Liang et al., 2013), demonstrating the influence of Gangu inoculum on epidemics of neighboring regions. The above examples showed that the oversummering inoculum from Gangu could serve as important inoculum sources affecting epidemics of other regions in China. Additionally, the result of this study for *Pst* was consistent with the previous findings that the population genetic diversity of *Pst* in Tianshui (Zheng et al., 2005) and Longnan regions (Lu et al., 2009) was much higher in higher-altitude than in lower-altitude area. This implied that the dispersal may occur from high altitude to low altitude. As to *Bgt*, however, there were no study and similar demonstration on spore dispersal in this region.

The main trend of pathway of *Pst* from source region to target regions is basically clear (Zeng and Luo, 2006). Although such pathway of *Bgt* is not as clear as that of *Pst*, the importance of oversummering inoculum on epidemics in local and adjacent regions for both diseases is inferred through this study. It might not be easy to estimate how large area that the data from spore traps could represent the inoculum in the fields to estimate the risk of disease epidemics. However, efficient disease management strategies in Gangu could significantly reduce the amount of inoculum in source region and to decrease the risk of epidemics in other regions. Such strategies may include cultivation of resistant varieties different from other regions, chemical control to reduce airborne spores, removal/management of alternate hosts, accurate estimation of the spore concentration periodically to predict the possible risk of epidemics, and monitoring of dynamics of races of both pathogens.

Acknowledgements

This study was supported by the National Natural Science Foundation of China (31371881), and the National Key Research and Development Program of China (2016YFD0300702, 2016YFD0201302).

Appendix A. Supplementary data

Supplementary data related to this article can be found at http://dx.doi.org/10.1016/j.cropro.2018.03.005.

References

Aylor, D.E., 1993. Relative collection efficiency of Rotorod and Burkard spore samplers for airborne *Venturia inaequalis* ascospores. Phytopathology 83, 1116–1119.
Bernal-martínez, L., Buitrago, M.J., Castelli, M.V., Rodríguez-Tudela, J.L., Cuenca-Estrella, M., 2012. Detection of invasive infection caused by *Fusarium solani* and non-*Fusarium solani* species using a duplex quantitative PCR-based assay in a murine model of fusariosis. Med. Mycol. 50, 270–275.
Cao, S., Luo, H., Jin, S., Duan, X., Zhou, Y., Jin, M., Jia, Q., 2011. Over-summering of *Blumeria graminis* f. sp. *tritici* in Tianshui of Gansu and effects of the sexual stage on infection cycle. Plant Prot. 37, 115–119.
Cao, X., Yao, D., Xu, X., Zhou, Y., Ding, K., Duan, X., Fan, J., Luo, Y., 2015. Development of weather- and airborne inoculum-based models to describe disease severity of wheat powdery mildew. Plant Dis. 99, 395–400.
Cao, X., Yao, D., Zhou, Y., West, J., Xu, X., Luo, Y., Ding, K., Fan, J., Duan, X., 2016. Detection and quantification of airborne inoculum of *Blumeria graminis* f. sp. *tritici* using quantitative PCR. Eur. J. Plant Pathol. 146, 225–229.
Chen, W., Wellings, C., Chen, X., Kang, Z., Liu, T., 2014. Wheat stripe (yellow) rust caused by *Puccinia striiformis* f. sp. *tritici*. Mol. Plant Pathol. 15, 433–446.
Chen, X., 2005. Epidemiology and control of stripe rust [*Puccinia striiformis* f. sp. *tritici*] on wheat. Can. J. Plant Pathol. 27, 314–337.
Dedeurwaerder, G., Duvivier, M., Mvuyenkure, S.M., Renard, M.E., Van Hese, V., Marchal, G., Moreau, J.M., Legrève, A., 2011. Spore traps network: a new tool for predicting epidemics of wheat yellow rust. Commun. Agric. Appl. Biol. Sci. 76, 667–670.
Duvivier, M., Dedeurwaerder, G., Proft, M.D., Moreau, J.M., Legrève, A., 2013. Real-time PCR quantification and spatio-temporal distribution of airborne inoculum of *Mycosphaerella graminicola* in Belgium. Eur. J. Plant Pathol. 137, 325–341.
Kennedy, R., Wakeham, A.J., 2015. Measuring biological particles in the air using the Hirst type spore trap: aerobiology in the age of genomics. Ann. Appl. Biol. 166, 1–3.
Li, B., Cao, X., Chen, L., Zhou, Y., Duan, X., Luo, Y., Fitt, B.D.L., Xu, X., Song, Y., Wang, B., Cao, S., 2013. Application of geographic information systems to identify the over-summering regions of *Blumeria graminis* f. sp. *tritici* in China. Plant Dis. 97, 1168–1174.
Li, Y., Gu, Y., Wu, B., Jin, S., Cao, S., Wang, X., Sun, Z., Luo, Y., Ma, Z., 2015. Establishment of a duplex *Taq*Man real-time PCR method for quantifying *Puccinia striiformis* f. sp. *tritici* and *Blumeria graminis* f. sp. *tritici*. Acta Phytopathol. Sin. 45, 205–210.
Li, Z., Zeng, S., 2002. Wheat Rust in China. China Agricultural Press, Beijing, pp. 379.
Liang, J., Liu, X., Li, Y., Wan, Q., Ma, Z., Luo, Y., 2016. Population genetic structure and migration of *Puccinia striiformis* f. sp. *tritici* between Gansu and Sichuan Basin populations of China. Phytopathology 106, 192–201.
Liang, J., Wan, Q., Luo, Y., Ma, Z., 2013. Population genetic structures of *Puccinia striiformis* in Ningxia and Gansu provinces of China. Plant Dis. 97, 501–509.
Limpert, E., Godet, F., Müller, K., 1999. Dispersal of cereal mildews across Europe. Agric. For. Meteorol. 97, 293–308.
Liu, M., McCabe, E., Chapados, J.T., Carey, J., Wilson, S.K., Tropiano, R., Redhead, S.A., Lévesque, C.A., Hambleton, S., 2015. Detection and identification of selected cereal rust pathogens by TaqMan® real-time PCR. Can. J. Plant Pathol. 37, 92–105.
Liu, W., Shao, Z., 1998. Analysis on climatic factor for epidemiology of wheat powdery mildew in China. Plant Prot. Technol. Extens. 18, 3–5.
Liu, Y., Tang, Q., 1985. The role of the asexual stage of wheat powdery mildew *Erysiphe graminis* f. sp. *tritici* played in the cycle of infection. Acta Phytopathol. Sin. 15, 191–192.
Lu, N., Wang, J., Zhan, G., Huang, L., Kang, Z., 2009. SSR analysis of population genetic diversity of *Puccinia striiformis* f. sp. *tritici* in dfferent altitude regions of Longnan, Gansu. Mycosystema 28, 496–503.
Luo, Y., Ma, Z., Reyes, H.C., Morgan, D., Michailides, T.J., 2007. Quantification of airborne spores of *Monilinia fructicola*, in stone fruit orchards of California using real-time PCR. Eur. J. Plant Pathol. 118, 145–154.
Meitz-Hopkins, J.C., Diest, S.G.V., Koopman, T.A., Bahramisharif, A., Lennox, C.L., 2014. A method to monitor airborne *Venturia inaequalis* ascospores using volumetric spore traps and quantitative PCR. Eur. J. Plant Pathol. 140, 527–541.
Nagarajan, S., Singh, H., Joshi, L.M., Saari, E.E., 1977. Prediction of *Puccinia graminis*, f.

sp. *tritici*, on wheat in India by trapping the uredospores in rain samples. Phytoparasitica 5, 104–108.
Shang, H., Ren, W., Wang, S., 1990. The discussion of a grading standard of wheat stripe rust severity. Plant Prot. 16, 31.
Sheng, B., Duan, X., 1991. Improvement of scale 0-9 method for scoring adult plant resistance to powdery mildew of wheat. Beijing Agri. Sci. 9, 38–39.
Wan, A., Chen, X., He, Z., 2007. Wheat stripe rust in China. Aust. J. Agric. Res. 58, 605–619.
Wan, A., Zhao, Z., Chen, X., He, Z., Jin, S., Jia, Q., Yao, G., Yang, J., Wang, B., Li, G., 2004. Wheat stripe rust epidemic and virulence of *Puccinia striiformis* f. sp. *tritici* in China in 2002. Plant Dis. 88, 896–904.
Wan, Q., Liang, J., Luo, Y., Ma, Z., 2015. Population genetic structure of *Puccinia striiformis* in northwestern China. Plant Dis. 99, 1764–1774.
West, J.S., Atkins, S.D., Fitt, B.D.L., 2009. Detection of airborne plant pathogens; halting epidemics before they start. Outlooks Pest Manag. 20, 11–14.
West, J.S., Kimber, R.B.E., 2015. Innovations in air sampling to detect plant pathogens. Ann. Appl. Biol. 166, 4–17.
Yang, L., Sun, L., Ruan, X., Qiu, D., Chen, D., Cai, X., Li, H., 2015. Development of a single-tube duplex real-time fluorescence method for the rapid quantitative detection of *Fusarium oxysporum* f. sp. *cubense* race 1 (FOC1) and race 4 (FOC4) using TaqMan probes. Crop Protect. 68, 27–35.
Zadoks, J.C., Chang, T.T., Konzak, C.F., 1974. A decimal code for the growth stages of cereals. Weed Res. 14, 415–421.
Zeng, S., Luo, Y., 2006. Long-distance spread and interregional epidemics of wheat stripe rust in China. Plant Dis. 90, 980–988.
Zeng, X., Luo, Y., Zheng, Y., Duan, X., Zhou, Y., 2010. Detection of latent infection of wheat leaves caused by *Blumeria graminis* f. sp. *tritici* using nested PCR. J. Phytopathol. 158, 227–235.
Zhang, Z., Li, Z., 1991. The laws of occurence and development of powdery mildew of wheat in Tianshui area. J. N.W. Sci-Tech Uni. Agri. Fore. 19, 81–86.
Zhao, J., Wang, L., Wang, Z., Chen, X., Zhang, H., Yao, J., Zhan, G., Chen, W., Huang, L., Kang, Z., 2013. Identification of eighteen *Berberis* species as alternate hosts of *Puccinia striiformis* f. sp. *tritici* and virulence variation in the pathogen isolates from natural infection of barberry plants in China. Phytopathology 103, 927–934.
Zheng, W., Chen, S., Kang, Z., Wang, Y., Wu, L., Li, Z., 2005. DNA fingerprinting of natural population of *Puccinia striiformis* f. sp. *tritici* in Tianshui area. Mycosystema 24, 199–206.
Zheng, Y., Luo, Y., Zhou, Y., Zeng, X., Duan, X., Cao, X., Song, Y., Wang, B., 2013. Real-time PCR quantification of latent infection of wheat powdery mildew in the field. Eur. J. Plant Pathol. 136, 565–575.